Miltefosine inhibits the membrane remodeling caused by phospholipase action by changing membrane physical properties

Yenisleidy de las Mercedes Zulueta Díaz, Ernesto Esteban Ambroggio, María Laura Fanani

PII: S0005-2736(20)30249-2

DOI: https://doi.org/10.1016/j.bbamem.2020.183407

Reference: BBAMEM 183407

To appear in: *BBA - Biomembranes*

Received date: 25 April 2020

Revised date: 23 June 2020

Accepted date: 29 June 2020

Please cite this article as: Y. de las Mercedes Zulueta Díaz, E.E. Ambroggio and M.L. Fanani, Miltefosine inhibits the membrane remodeling caused by phospholipase action by changing membrane physical properties, *BBA - Biomembranes* (2020), https://doi.org/10.1016/j.bbamem.2020.183407

Miltefosine inhibits the membrane remodeling caused by phospholipase action by changing membrane physical properties

Yenisleidy de las Mercedes Zulueta Díaz [a,b], *Ernesto Esteban Ambroggio* [a,b] *and María Laura Fanani* [a,b]*

[a] Departamento de Química Biológica Ranwel Caputto, Facultad de Ciencias Químicas, Universidad Nacional de Córdoba, Córdoba, Argentina.

[b] Centro de Investigaciones en Química Biológica de Córdoba (CIQUIBIC), CONICET, Haya de la Torre y Medina Allende, Ciudad Universitaria, X5000HUA, Córdoba, Argentina.

* Corresponding author: María Laura Fanani, lfanani@fcq.unc.edu.ar; tel +54-351-5353458.

Abstract: Miltefosine (hexadecylphosphocholine or HePC) is an alkylphosphocholine approved for the treatment of visceral and cutaneous Leishmaniasis. HePC exerts its effect by interacting with lipid membranes and affecting membrane-dependent processes. The molecular geometry of HePC suggests that the pharmacological function of HePC is to alter membrane curvature. As a model system, we studied the enzyme production in model membranes of diacylglycerol (DAG) or ceramide (CER), lipids involved in cell signaling which alter the structure of membranes. Here, we studied the effect of HePC on changes in phospholipase activity and on the effect that the lipid products have on the curvature and fusogenicity of membranes where they accumulate. Our results indicate that HePC inhibits the long-time restructuring of membranes, characteristic of the DAG and CER enzyme formation processes. In addition, the drug also reduces the fusogenicity of phospholipase-derived products. We postulate that the effect of HePC is due to a non-specific geometric compensation of HePC to the inverted cone-shape of DAG and CER products, acting as a relaxation agent of membrane curvature stress. These data are important for understanding the

mechanism of action by which HePC regulates the lipid metabolism and signal transduction pathways in which these enzymes are involved.

Keywords: alkylphospholipids, phospholipase C, sphingomyelinase; lipid membrane curvature, liposome aggregation, liposome fusion.

Abbreviations: DOPC: dioleoylphosphatidylcholine; DOPE: dioleoylphosphatidylethanolamine; POPC: 1-palmitoyl-2-oleoyl-glycero-3-phosphocholine, DAG: diacylglycerol; CER: ceramide; SM: sphingomyelin; HePC; Hexadecylphosphocholine or miltefosine, SMase: sphingomyelinase; PLC: Phospholipase C; TLC: thin-plate chromatography, DLS: dynamic light scattering; GUVs: giant unilamellar vesicles; LUVs: large unilamellar vesicles.

1. Introduction

Miltefosine or hexadecylphosphocholine (HePC) is an alkyllysophospholipid analog. Along with other alkylphospholipid analog members, HePC was originally developed as an antitumor agent in the late 1980s. Even after HePC was approved for the treatment of cutaneous metastases in breast cancer patients, it was found clinically ineffective [1]. However, further studies demonstrated that HePC is active against most *Leishmania* species, including those that cause cutaneous disease. HePC, sold under the trade name Impavido® among others**,** is used against the cutaneous, mucosal and visceral forms of Leishmaniasis in different countries [1–5]. This treatment shows several side effects including vomiting, abdominal pain, fever, headaches, and decreased kidney function. Currently, HePC–based treatments are studied in 42 clinical trials reported in the U.S. National Library of Medicine (NLM-NIH) (ClinicalTrials.gov). 38 of them are for less aggressive treatment of Leishmaniasis in its different forms, and one for cancer therapy.

HePC mechanism of action against both *Leishmania* parasites and human cancer cells links its activity mainly to (i) apoptosis and (ii) disturbance of lipid-dependent cell signaling pathways[5]. In all cases, HePC action involves insertion into the plasma membrane as a prerequisite for drug uptake before the active molecule reaches its intracellular targeting. In mammalian cell cultures, HePC is most effective in metabolically active, proliferating cells, such as cancer cells, but not in quiescent normal cells [2]. HePC is active against most species of *Leishmania*, but not all [5]. At plasma membrane level, *L. donovani*, the causative species on the Indian subcontinent and in eastern Africa, show a prevalence of phosphatidylethanolamine (PE) over phosphatidylcholine (PC) and sphingomyelin (SM) [6]. This contrast with the occurrence in the mammalian cells plasma membrane, where PC prevails over SM and PE [7]. Notably, a transient treatment of *Leishmania* parasites with HePC enhances the PE and reduces PC content in the plasma membrane.

HePC affects the biosynthesis of PC by inhibiting the rate-limiting enzyme CTP:phosphocholine cytidylyltransferase (CT) and altering intracellular cholesterol traffic and metabolism in human tumor cell lines [2,4,6,8]. HePC was also responsible for an apoptosis-like death in *L. donovani*, both in the promastigotes and amastigotes forms [9]. This drug interferes with phospholipid metabolism that is differentially expressed in HePC-susceptible and HePC-resistant *L. donovani* [10]. Different than mammalian cells, cholesterol is not biosynthesized in *Leishmania* parasites, which have to take it up from the external medium. Ergosterol, is also present in *Leishmania* membranes, due to biosynthesis. Total sterols account for as much as 43.3 % w/w of neutral lipids [11]. It has been reported that HePC has strong affinity for sterols [9,12,13] and HePC transiently treated parasites show an increase in its cholesterol content [6]. It is worth noting that both lipids increased after HePC transient treatment (PE and cholesterol) have in common its capacity for promoting non-lamellar lipid phases [14,15].

Early reports demonstrated that the activity of several enzymes of central relevance in lipid homeostasis and cell signaling are highly regulated by the presence of non-lamellar forming lipids. An increase in the content of the nonlamellar-phase prone lipids PE or diacylglycerol (DAG) on

lipid membranes triggers the binding of several cytosolic proteins, whose membrane forms are metabolically active. The mechanism governing this effect correlates with an increase in the membrane's stored curvature and responds to an increased surface hydrophobicity and dehydration [16–18]. This is the case of CT and DAG kinase [16,19,20], protein kinase C [17,21], G protein [22–24], and other important enzymes that regulate lipid metabolism, including several phospholipases [19,25,26]. In this context, it is conceivable that specific therapies could be designed on the basis of regulating membrane lipid structure [15]. Destabilization of nonlamellar membrane structures by the cytotoxic drug daunomycin has been demonstrated to promote G-protein and PKC dissociation from the plasma membrane and disruption of cellular signaling pathways [27].

It was proposed that HePC acts on CT activity by disrupting membrane curvature elastic stress and inhibiting membrane-associated protein activity. Dymond et al. [28] evaluated the structure-activity relationship of alkyllysophospholipids from the literature and provided a theoretical framework for the hypothesis, which predicts that the most potent alkyllysophospholipid analogs will be in the type I lipid group. Type I lipids form aggregates whose polar–apolar interface curves away from the aqueous domains, which is commonly reported as "positive" curvature structures, like micelles. HePC shows a cone-like shape and was determined to belong to type I, favoring micelles and small lamellar structures [12,28]. On the other hand, inverted-cone lipids (e.g. PE) forms non-lamellar structures with "negative" curvature, such as hexagonal o cubic phases [14]. The combination of both groups of non-lamellar prone lipids (conic and inverted-conic shaped) would compensate their geometric constrains stabilizing planar lamellar phases. Direct evidence of the HePC capacity of perturbing highly "negative" curved lipid structures has been provided by Malheiros [29]. In this thesis, the addition of only 5 % w/w of HePC to cubosomes disrupts its cubic crystalline structure.

Previous reports from our laboratory and others [12,30–32] demonstrate that the incorporation of HePC into the lipid interface results in changes of the physical properties of the host membrane. In the present work, we test the capacity of HePC to alter the high curved membrane structures

induced by the enzyme production of DAG and ceramide (CER), both cataloged as lamellar disrupting lipids. These important lipid second messengers are produced by the action of phospholipase C (PLC) and sphingomyelinase (SMase), respectively, and have an inverted-cone geometry. Their membrane accumulation induces the restructuring of the lipid bilayers into aggregates containing non-lamellar structures with high surface curvature [26,33–36], affecting various cellular processes including those that involves membrane fusion [16,37]. Furthermore, direct evidence has been reported that enzymatically-induced changes in lipid composition regulate the fusion between the plasma membrane and liposomes [38]. In turn, those changes in curvature stress have the potential to affect the action of other important actors in lipid metabolism and signaling, as described above [16,19–22,24,39–41].

Enzymes related to lipid metabolism, such as phospholipases, are very susceptible to changes in the physical properties of the membrane and, in turn, indirectly transmit information to other metabolic pathways through structural and electrostatic changes or phase state alterations of the biomembranes in which they act [33,41–44]. Based on these reports, here we study the effect of HePC on phospholipase enzyme activity and on the membrane physical property changes that the phospholipase products induce. Our hypothesis is that the membrane insertion of the amphiphilic cone-shaped alkylphospholipid HePC either directly modulates membrane curvature or compensates the stress generated by the inverted-cone shaped lipids produced by PLC or SMase. We thus address not only the biochemical but also the biophysical changes that HePC exerts when present in lipid membranes. Our results aid the understanding of the mechanism of action by which HePC regulates the lipid metabolism and signal transduction pathways.

2. Materials and methods

2.1. Chemicals and reagents

Miltefosine or Hexadecylphosphocholine (HePC), 1,2-dioleoyl-sn-glycero-3-phosphocholine (DOPC), 1-palmitoyl-2-oleoyl-glycero-3-phosphocholine (POPC), 1,2-dioleoyl-sn-glycero-3-phosphoethanolamine (DOPE) and Sphingomyelin (Brain, Bovine) (SM) were purchased from Avanti Polar Lipids, Inc. (Alabama, U.S.A.). Fluorescent probes 1,2-dioleoyl-sn-glycerol-3-phosphoethanolamine-N-lysamine rhodamine B sulfonyl) (ammonium salt) (Rho-PE) and phosphatidylethanolamine-N- (7-nitro-2-1,3-benzoxadiazol-4-yl) (NBD-PE) were from Avanti Polar Lipids, Inc. (Alabama, U.S.A.). For enzyme activity studies, the enzymes sphingomyelinase (SMase) from *Bacillus cereus* (EC 3.1.4.12) and phospholipase C (PLC) from porcine pancreas (EC 3.1.1.4) were used. Both were purchased from Sigma-Aldrich (St. Louis, MO). All other reagents, chloroform, methanol, acetic acid, sodium chloride, Tris-Base and HPTLC (high-performance thin-layer chromatography) silica gel 60 aluminum plates (Kieselgel 60), were purchased from Merck (Darmstadt, Germany). Hexane and petroleum ether were from Sintorgan (Argentina). All reagents were analytical grade (99% Pure) and used without further purification. Deionized water, with a resistivity of ~ 18 MΩ cm, was obtained from a Milli-Q Gradient System (Millipore, Bedford, MA).

2.2 Methods

2.2.1 Vesicles preparation

Multilamellar vesicles (MLVs) containing SM:DOPE (70:30 molar ratio) or DOPC:DOPE (80:20 molar ratio) were used in the absence and presence of 20 mol% of HePC. The MLVs were prepared by generating a uniform lipid film on the wall of a glass test tube. For this, 160 nmol of lipid or lipid/HePC mixtures were placed into glass tubes from a chloroform lipid solution and drayed by solvent evaporation under an N_2 (g) stream. Traces of solvent were removed during 2 h treatment in a high vacuum chamber. The lipids were hydrated with 400 μL of a buffer solution containing 10 mM HEPES, 200 mM NaCl, 10 mM $CaCl_2$, at pH 7 for PLC studies and with the addition of 2 mM $MgCl_2$ for SMase. The samples were vigorously mixed for two min and subjected to five freeze-thaw cycles (−195°C in liquid nitrogen and 60°C in a heating bath, respectively). Each procedure

was maintained for 2 min. Large unilamellar vesicles (LUVs) were prepared by extrusion (21 times) of MLVs through polycarbonate filters of 100 nm pore size at 45°C. The liposomes samples were kept at room temperature (22±2°C) and used within 8 h. For fluorescent measurements, appropriate aliquots of the fluorescent probe Rho-PE were added to the chloroform lipid suspension, reaching 1 mol%.

GUVs were prepared by electroformation. Briefly, 7 μL of a lipid (POPC or bbSM) or lipid/HePC solution (0.5 mg/mL in chloroform: methanol 2:1 v/v), doped with 1 mol% of the fluorescent probe NBD-PE, were spread onto two stainless steel plates as described in the Ref. [45]. The plates were subjected to vacuum (1 h) to remove any remaining traces of organic solvent. The lipids were hydrated with a 300 mOsm sucrose solution previously filtered and heated to 60°C. The electrodes were connected to a homemade function generator applying potential for 1 h at 37°C for POPC or 2 h at 60°C for bbSM vesicles, respectively. Initially, a sine wave potential of 10 Hz was applied, with amplitude from 0 to 2.6 V peak-to-peak potential increasing linearly in 60 s (Bartlett modulation), which was afterward maintained at 2.6 V peak-to-peak potential [45].

2.2.2 Enzyme Activity

LUVs containing DOPC:DOPE (80:20 molar ratio) or SM:DOPE (70:30 molar ratio) in the absence and presence of 20 mol% of HePC to reach a 400 μM total lipid concentration, were incubated with PLC (7.5×10^{-3} U/ml) or *Bacillus cereus* SMase (1.4 U/mL) at 37°C. For temperature and stirring control, a Quantum Northwest (Liberty Lake, WA) TC 125 temperature controller system was used. Aliquots of this suspension were taken at regular intervals and chloroform:methanol (2:1) was added. The lower phase of the extraction system was evaporated, and the samples subjected to TLC. Chloroform:methanol:water (100:42:6, v/v/v) was run up to approximately one-third of the plates to separate PC from SM, and, after drying the plates, chloroform:methanol:acetic acid (96:4.1, v/v/v) was run up to the top of the plates to isolate the CER. For PLC the same procedure was used, but using chloroform:methanol:water (60:30:5 v/v/v) to separate DOPC and DOPE, and further

treatment with hexane:ethyl ether:acetic acid (80:20:2 v/v/v) was necessary to separate DAG. For lipid identification and quantification, the plates were submerged into an aqueous solution of 3% p/v cupric acetate, 8% v/v phosphoric acid and heated up to 90°C. Lipid semi-quantification was performed using the ImageJ 1.43u program (NIH).

2.2.3 Effects of phospholipases on vesicle size

Spectrophotometry and vesicle size distribution data were obtained using LUV preparations containing SM:DOPE or DOPC:DOPE in the absence or presence of 20 mol% of HePC, as described above. Samples were taken immediately before (t=0) and at specified incubation times after phospholipase addition. The absorbance of each sample was measured using a UV-visible spectrophotometer (Shimadzu UV-2401PC). Absorbance curves vs. time were measure at λ = 500 nm with a slit width of 1 nm at 37°C.

Changes in vesicle size distribution profiles resulting from PLC or SMase action were followed by dynamic light scattering (DLS) analysis, using a Submicron Particle Sizer (Nicomp 380, Santa Barbara, CA). Before enzyme treatment, LUV preparations showed a bell-shape size distribution centered at ~100 nm. Particle size distribution profiles were traced at the different incubation times after PLC or SMase addition. The percentage of the volume of lipid particles larger than 250 nm was calculated from size distribution tracings by relating the peak areas corresponding to lipid particle populations greater than 250 nm to the total area.

2.2.4 Confocal microscopy visualization of giant unilamellar vesicles (GUVs)

A small aliquot of the GUV suspension (50 μL) was transferred to an 8-well observation chamber (Lab-Tek, Thermo Fisher Scientific, Inc.NYSE:TMO) and diluted with 300 mOsm 10mM HEPES, 200mM NaCl, 10mM $CaCl_2$, 2mM $MgCl_2$ or 10mM HEPES, 200mM NaCl, 10 mM $CaCl_2$ at pH 7 buffer for SMase or PLC experiments, respectively. The sucrose and buffer solutions were checked for isosmolarity with an Automatic Micro-Osmometer OM-806, (VOGEL GmbH & Co.KG,

Giessen, Germany). Before GUV addition to the well, the glass of the observation chamber was treated with a 10 mg/mL BSA solution, which prevented GUV rupture onto the slide. The excess of BSA was eliminated by several washes with buffer. The GUVs were observed with a fluorescence confocal microscope (Olympus FV 1000, Tokyo, Japan) with a 60x oil objective.

For experiments to study the fusion of LUVs to GUVs, the GUVs in sucrose/buffers were mixed with the LUV suspension 2:1 (v/v) and this was left for 10 min before imaging by confocal fluorescence microscopy. GUVs doped with NBD-PE and LUVs doped with Rho-PE were visualized and fluorescence energy transfer was detected by selecting three different imaging channels; (i) the direct donor (NBD-PE) excitation at 488 nm and emission at 500-545 nm, (ii) donor excitation at 488 nm and acceptor (DPPE-Rh) emission at 600-700 nm, and (iii) direct acceptor excitation at 543 nm and emission at 600-700 nm. The laser power was kept at a minimum to allow a sufficient signal while avoiding bleaching. Confocal Images of GUVs were processed and quantified with the FIJI ImageJ software (NIH, USA).

2.2.5. Statistical treatment

Results are expressed as the mean±standard error of the mean (SEM) for three different experiments. Statistical comparisons were calculated by Student's t-test using the GraphPad QuickCalcs Web site: http://www.graphpad.com/quickcalcs (GraphPad Software, San Diego, CA). Values of $P<0.05$ or $P<0.001$ were considered to be statistically significant.

3. Results

3.1. HePC does not directly affect the enzyme activity of phospholipases (PLC and SMase).

We first analyzed the effect of HePC on the enzyme activity of PLC and SMase at short times (initial velocity). The substrates used were LUVs composed of DOPC:DOPE or SM:DOPE to

evaluate PLC and SMase activity, respectively. Both enzyme actions were reported in the 1990s as resulting in membrane aggregation and restructuring due to the accumulation of products in the membrane as DAG (PLC) or Cer (SMase). Those effects were enhanced by the presence of the non-lamellar forming lipid PE [46,47].

The enzyme products were detected by TLC. When the LUVs composed of DOPC:DOPE were treated with PLC, the presence of DAG appeared in the first 6 min and its progressive increase was achieved, reaching ~20 % of total DOPC hydrolysis both in the absence and presence of HePC (Figure 1A). Also, reaction rates remained similar (no significant statistical difference, P>0.1) being 3.27±0.04 $U.ml^{-1}.min^{-1}$ (HePC absence) and 3.1±0.2 $U.ml^{-1}.min^{-1}$ (HePC presence).

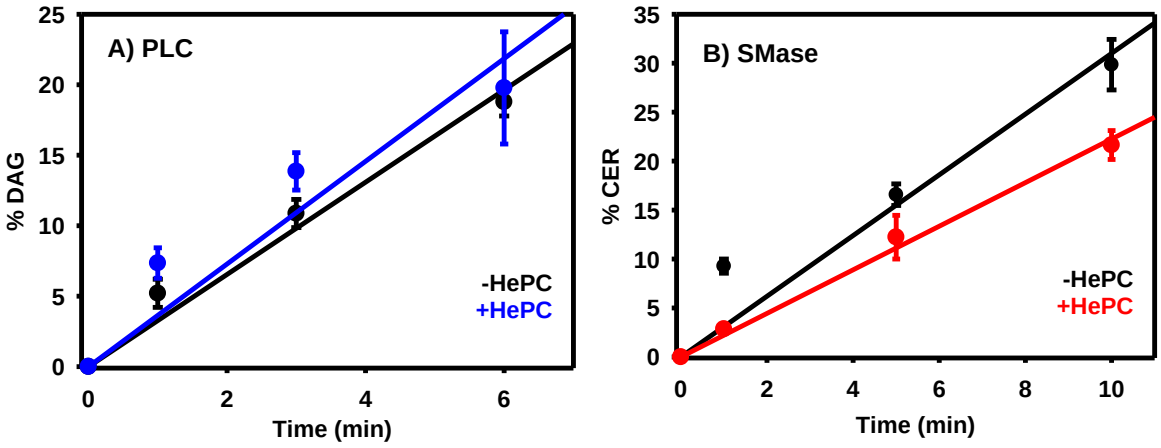

Figure 1: Reaction course of the enzymatic production of diacylglycerol (DAG) and ceramide (CER), determined by thin-layer chromatography (TLC). A) PLC-driven conversion of glycerophospholipids to DAG in liposomes containing DOPC:DOPE (80:20 molar ratio) with or without the addition of 20 mol% of HePC. B) SMase-driven conversion of sphingomyelin (SM) to CER in liposomes containing SM:DOPE (70:30 ratio) with or without the addition of 20 mol% of HePC. A final lipid concentration of 0.4 mM was used. PLC (3×10^{-4} U / ml) or SMase (2.8×10^{-2} U / ml) were added at t = 0. Incubation proceeded at 37°C for the indicated intervals, until stopped by the addition of the solvents required for lipid extraction. Experimental data correspond to the formation of DAG or CER in the absence (black symbols) and presence of HePC (open symbols, respectively). Error bars correspond to SD of a triplicate experiment.

A similar situation was observed for SMase activity on SM:DOPE LUVs. The formation of CER (Figure 1B) reached 20 - 30% of product formation in the first 10 minutes of the reaction. The reaction rates obtained were 3.1±0.2 and 2.2±0.1 ($U.ml^{-1}.min^{-1}$) in the absence and presence of HePC, respectively. This indicates a statistically significant inhibition (29%; $P<0.05$) of the reaction rate by HePC.

3.2. HePC inhibits PLC and SMase induced liposome fusion

We explored the capacity of HePC to alter the highly curved membrane structures induced by the DAG and CER lipids. Such inverted-cone-shaped lipids are produced by the action of PLC or SMase on the outer hemilayer of the liposomes. Therefore, the lipid products accumulate asymmetrically in the membrane until the flip-flop process dissipates this translayer concentration gradient. Flip-flop rates for CER and DAG are in the order of ms or longer, and are somewhat greater for DAG than for CER [48]. Therefore, this process is on a similar time scale to that of the phospholipase constant rates [49,50]. This induces transient lateral curvature stresses at the membrane, which relax by restructuring the membrane through processes like fusion or aggregation where a non-lamellar intermediate occurs [34,35,51,52].

In this section, liposome fusion/aggregation processes after enzyme treatment were indirectly assessed by turbidimetry. This effect responds to an increase in lipid particle size (from ~ 100 nm diameter to micrometric-size particles) that increases dispersion of light at 500 nm. Therefore, we analyzed the lipid particle size change by dynamic light scattering (DLS).

When PLC is added to LUVs composed of DOPC:DOPE, an increase in turbidity is observed concomitant to DAG production (Figure 2A).

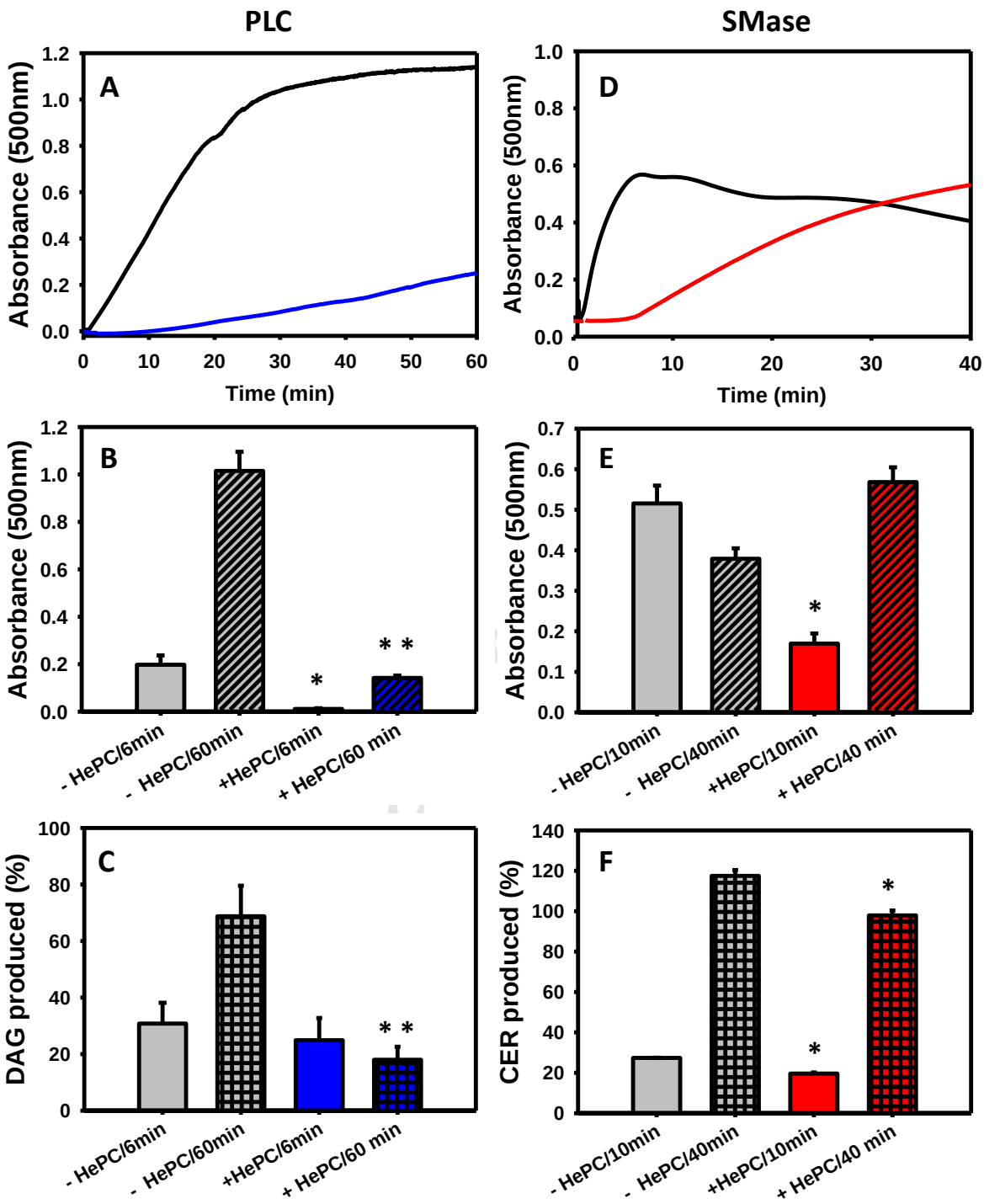

Figure 2: PLC or SMase action on vesicle aggregation. Vesicle restructuring was evidenced by the turbidimetry method obtaining absorbance curves vs time. (A, D) Liposome aggregation curves (~100 nm diameter) composed of DOPC:DOPE or SM:DOPE were exposed to PLC (7.5 x 10^{-3} U / ml) (A) or SMase (1.4 U / ml) (D) at 37° C in absence (black line) and presence (blue or red line)

of 20 mol% of HePC. The curves in A and D are representative of triplicate experiments. (B, E) Comparison of absorbance values obtained at the indicated times after enzyme addition in the absence (gray bars) and presence (blue or red bars) of HePC. (C, F) Quantification of DAG or CER enzyme formation in the absence (gray bars) and presence of 20 mol% of HePC (blue and red bars, respectively). In all cases, the total lipid concentration was 0.4 mM. The experiments were performed in triplicate, average values ±SEM (n = 3). Asterisks indicate statistical differences of data obtained in similar conditions in the absence and presence of HePC with P <0.05 (*) or P <0.0001 (**).

This effect was first observed in the early 1990s by Felix Goñi et al. and was interpreted in terms of liposome aggregation and fusion [46,47]. The addition of 20 mol% of HePC to our system clearly showed a drastic decrease in vesicle aggregation, evidenced by a slower absorbance increase observed after enzyme addition (Figure 2A). This effect was quantified at 6 and 60 min, showing a decrease in absorbance in the presence of HePC of 95 and 82%, respectively, in comparison to conditions in the absence of the drug (Figure 2B).

Additionally, there were no significant differences in the amount of DAG formation at 6 min in the absence and presence of HePC (Figure 2C and 1A). This demonstrates that, even when a similar amount of DAG is produced, HePC is impairing liposome fusion/aggregation. On the other hand, after 60 min of enzyme treatment, DAG production was reduced to a fourth (from 68±9 % to 18±5 %, see Figure 2C), while vesicle aggregation, evidenced by an absorbance reduction, decreases to less than a sixth by the presence of HePC (from 1.02±0.08 to 0.14±0.01, see Figure 2B). Therefore, even when a significant amount of DAG is produced, its effect on membrane restructuring is still hampered by HePC.

Early reports demonstrated that full PLC activity requires the presence of membrane surface irregularities or defects induced by the product DAG causing vesicle aggregation [53]. Our results show that HePC inhibits PLC activity when studied over long periods, concomitantly with

inhibition of vesicle aggregation. Therefore, we infer that HePC acts indirectly on PLC activity by somehow relaxing the curvature stress induced by DAG and thus inhibits full PLC activity.

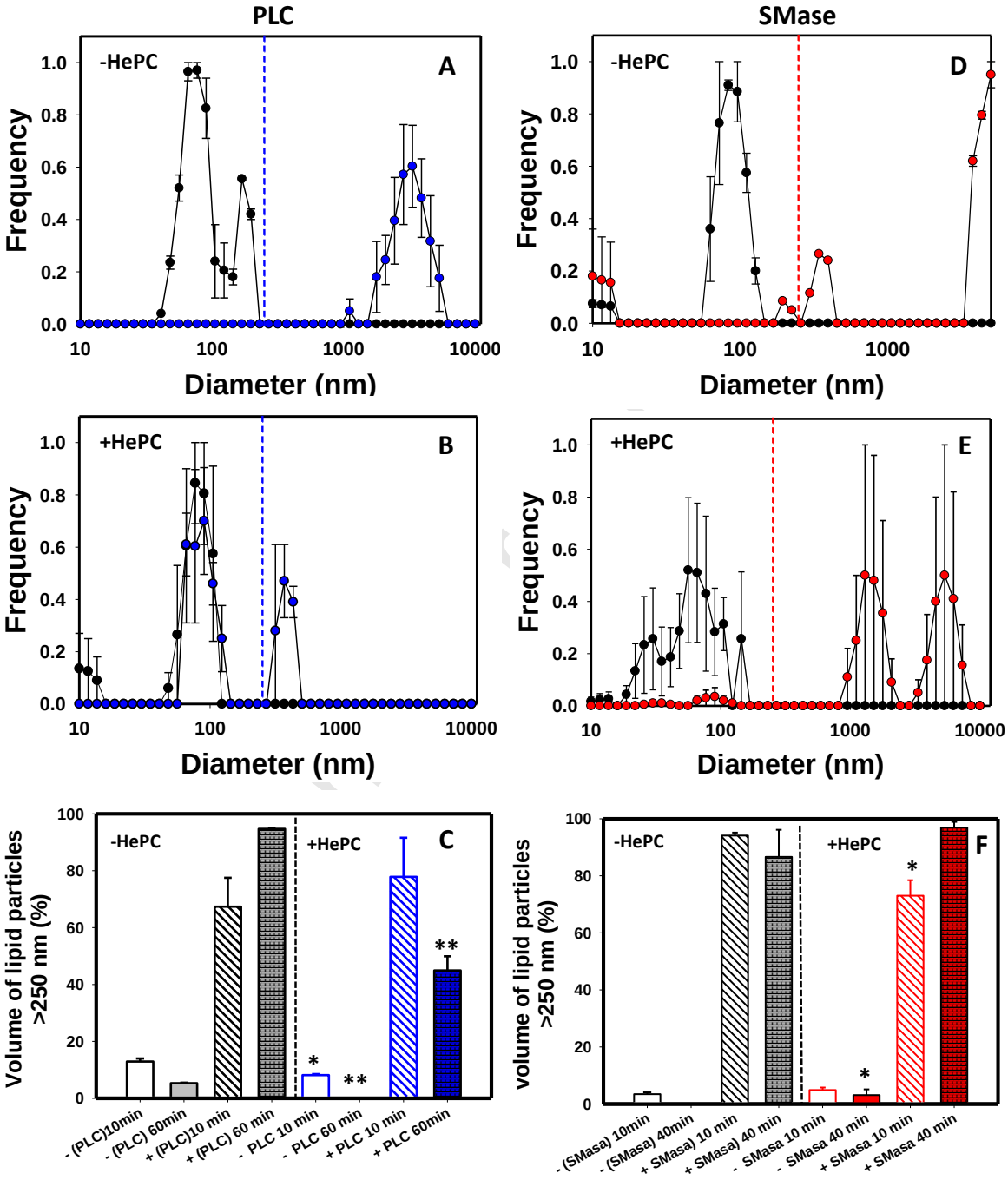

Figure 3: Changes in vesicle size distribution profiles as a consequence of PLC or SMase action followed by dynamic light scattering (DLS) analysis. Representative graphs of differences in the population size distribution of lipid particles that initially contained DOPC:DOPE (A, B) or

SM:DOPE (D, E) before (black symbols) and after 60 min of PLC or 40 min of SMase treatment (colored symbols). Comparison of the size distribution of LUVs in the absence (A, D) and the presence of 20 mol% HePC (B, E). The vertical dashed lines in A-B and D-E divide the particles smaller than the larger than 250 nm. The data is the average values ± SEM of triplicate experiments. (C, F) Analysis of the number of lipid particles larger than 250 nm as a percentage of the total population, calculated as the integral of the particle volume distribution curves vs diameter. Liposome and enzyme conditions are similar to those described in the legend of Figure 2. Asterisks in panels C and F indicate statistical differences of data with $P < 0.05$ (*) or $P < 0.0001$ (**).

The formation of large lipid particles by the action of PLC was confirmed by DLS (Figure 3A-C). Both vesicles, containing HePC or not, showed a particles population, with a size distribution centered at 100 nm before enzyme treatment (Figure 3A, black symbols). On the other hand, LUV suspensions containing HePC showed a small population close to 10 nm (corresponding to less than 8% of the total particle volume), which are HePC-enriched micelles (Figure 3B, black symbols) [12].

As can be observed from Figure 3, the liposomes of any composition were smaller than 250 nm before enzymatic treatment (black symbols in Figure 3A, B, D and E). Therefore, the occurrence of particles larger than 250 nm after the addition of enzymes has been taken as a consequence of liposome aggregation upon the generation of CER or DAG.

The enzyme production of DAG by PLC induced the appearance of a population of large particles (micrometric size), shifting the particle size distribution to a diameter range above 250 nm (Figure 3A, blue symbols). The presence of HePC reduces this effect (Figure 3B, blue symbols). A more detailed analysis shows that in the presence of HePC only~ 45% of the particle volume was organized in structures larger than 250 nm after treatment with PLC (Figure 3C). This matches the turbidity measurements, indicating that HePC reduces the vesicle aggregation process induced by the enzyme production of DAG.

Similar behavior was observed with the addition of SMase to liposomes of SM:DOPE in the absence and presence of HePC. There was an increase in turbidity over time (Figure 2D) with an abrupt increase in turbidity in the first 5 min of reaction in the absence of HePC, as reported before [46], and a further slow relaxation of the process (Figure 2D). The presence of HePC slows down the turbidity time-curve, reaching only a third of that observed in the absence of the drug at 10 min of reaction. Notably, over long periods the inverse relation is observed (Figure 2E), evidencing the occurrence of far-from-equilibrium processes related to vesicle aggregation that anneals over time.

The quantitative analysis of the extent of hydrolysis of SM in the absence and presence of HePC at 10 and 40 min is shown in Figure 2F. Both at short and long times, the presence of HePC induces up to 25% inhibition of the amount of CER formed. This shows that HePC affects SMase-dependent liposome aggregation to a greater extent than its enzyme activity. Therefore, HePC hinders the effect that CER exerts on the membrane physical properties, relaxing its curvature stress and fusogenicity, as will be discussed in the next section.

In the absence of SMase, the LUVs containing SM16:DOPE showed a population of vesicles with a diameter peak at 100 nm (Figure 3D, black symbols). Vesicles containing 20 mol% HePC also showed the presence of a smaller population of particles centered at 50 nm (Figure 3E, black symbols), in agreement with previous observations [12]. Enzyme hydrolysis of SM induced polydispersion in the particle distribution histogram, with a population larger than 250 nm both in the absence and in the presence of HePC (Figure 3D, E, red symbols). However, at short reaction times, the percentage of particle volume with a diameter larger than 250 nm is significantly smaller in the presence than in the absence of HePC (Figure 3F), confirming the turbidimetry assays. In summary, HePC slows down the aggregation of vesicles subjected to the rapid action of SMase at short times, probably because it relaxes the topographic frustration generated by CER by having a complementary symmetry. However, at long times, the action of SMase prevails and aggregated structures appear, which allow the evolution of catalysis to similar values to those obtained in the absence of HePC.

3.3. HePC inhibits LUV-GUV fusion

From the results shown in the previous section and bibliography data [35,36,46,53], we can conclude that vesicles containing enzymatically generated CER or DAG show fusogenic properties. Furthermore, these properties are inhibited by the presence of HePC. Taking into account that membrane fusion is at the heart of many essential cellular processes, such as intracellular trafficking and signaling via endo/lysosome fusion [51], and that those are proposed as target processes in HePC action [8], we further explored the effect of HePC on fusogenic liposomes, using giant unilamellar vesicles (GUVs) as a fusion target. Those micron-sized vesicles can be visualized directly under a fluorescence confocal microscope. They are flat at the molecular level, making them very useful mimics of the plasma membrane [51].

We performed a fusion assay by adapting the procedure described by Lira et al. [54]. In this system, LUVs, which are the substrate of the phospholipase, are labeled with the lipophilic probe NBD-PE and are mixed with Rho-PE-labeled GUVs designed as non-substrate. Vesicle fusion after enzyme addition is detected by two means: I) through the morphological changes of GUVs observed by confocal microscopy upon enrichment with the non-lamellar forming lipids DOPE and CER or DAG, and II) lipid mixing increases fluorescence resonance energy transfer (FRET) between the two probes and the red emission of the acceptor probe increases at expense of the emission of the donor (green), upon excitation of the donor probe.

GUVs composed of SM and labeled with the fluorescent probe NBD-PE were observed by confocal microscopy as circles when focused on the equatorial plane (Figure 4).

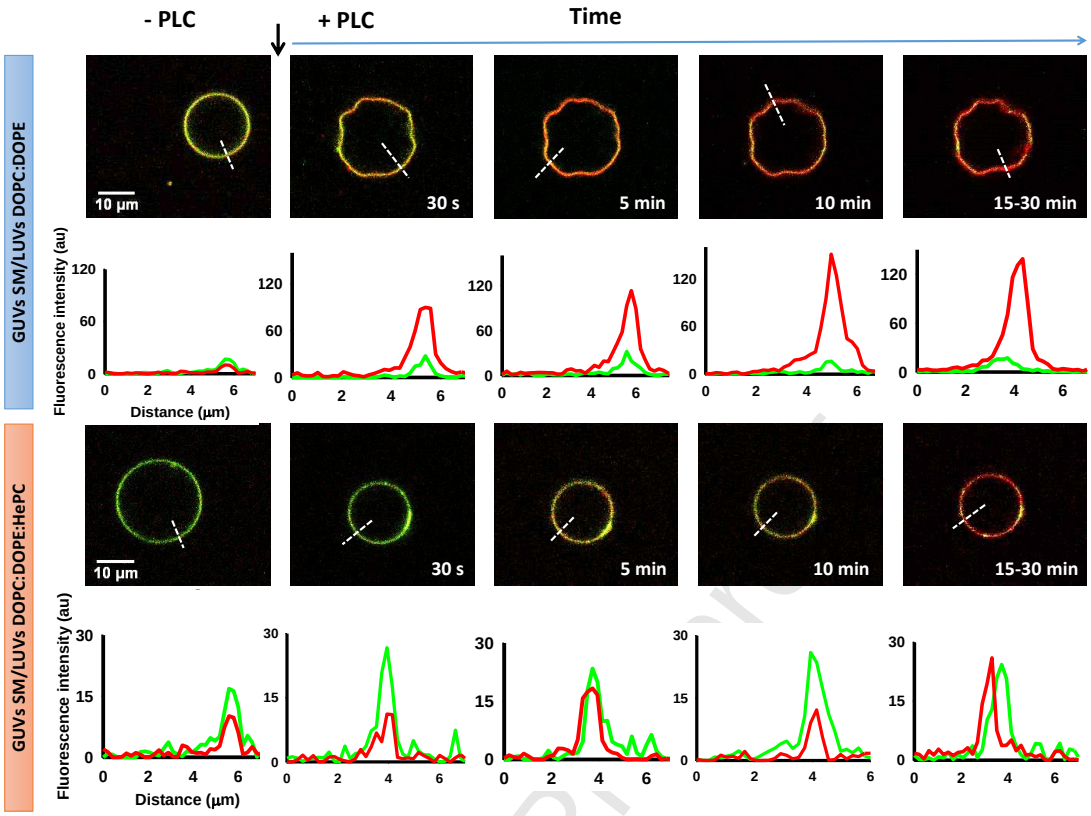

Figure 4: Confocal microscopy images of GUVs of SM labeled with NBD-PE (green) and fusogenic Rho-PE-labeled LUVs (red) composed of DOPC:DOPE (80:20) in the absence (upper panel) or presence (lower panel) of 20 mol% of HePC. The timestamps indicate the time after PLC addition. Fluorescence intensity profiles for the green and red channel in the GUV regions along the dashed lines are plotted under each image. Samples were excited at the NBD-PE excitation λ and images show the overlay of NBD-PE and Rho-PE emission channels.

LUVs composed of DOPC:DOPE:Rho-PE were used as the substrate of PLC. The addition of the enzyme to a LUV/GUV mixture triggered DAG formation in LUVs. Its fusion to the GUV membrane was evidenced by an increase in the red/green fluorescence ratio (increase in the FRET signal) at 30 min that doubled the initial value (Figure 6A). Concomitantly, changes in GUV shape were observed, which evidenced the occurrence of membrane areas with high curvature (see Figure 4). This may be explained by concentration of the non-lamellar forming lipids DOPE and DAG

originated in the PLC-treated LUVs. The changes in shape were observed in 94% of the GUVs analyzed (n=47) after 60 min of PLC treatment (see Figure S1 for image gallery and video_PLC in support information). Control experiments carried out in the presence of 100 mM EDTA, a condition where PLC is inhibited, did not show shape changes in GUVs (Figure S1).

When 20 mol% of HePC was present in the LUVs, their fusion to GUV membranes was reduced, as reflected by the low values of the red/green fluorescence ratio, which is statistically different than that observed in the absence of HePC (Figure 6A). As a consequence of the low extent of fusion and the presence of the cone-shaped HePC, GUVs incubated with this system showed no shape change (only 7% of non-circular GUVs were found, n= 85; see Figure 4 and video_PLC_HePC in support information).

GUVs formed by POPC and labeled with the fluorescent probe NBD-PE were observed by confocal microscopy as circles when focused on the equatorial plane (Figure 5). Liposomes composed of SM:DOPE:Rho-PE were used as the substrate of SMase. The addition of the enzyme to a LUV/GUV mixture triggers CER formation in LUVs. After a few minutes, red dots were observed attached to GUV (green) membranes (Figure 5 and video_SMase in support information).

This effect has been interpreted as liposome docking in a similar system [54]. In this stage, LUVs associated with but did not mix with the GUV lipid membrane. As the enzyme reaction progressed, the GUV membranes showed a significant increase in red fluorescent content (see Figure 6B) due to a burst in LUV fusion to GUVs, until GUVs collapsed in a non-lamellar lipid structure (Figure 5, upper panel, see also videos in support information).

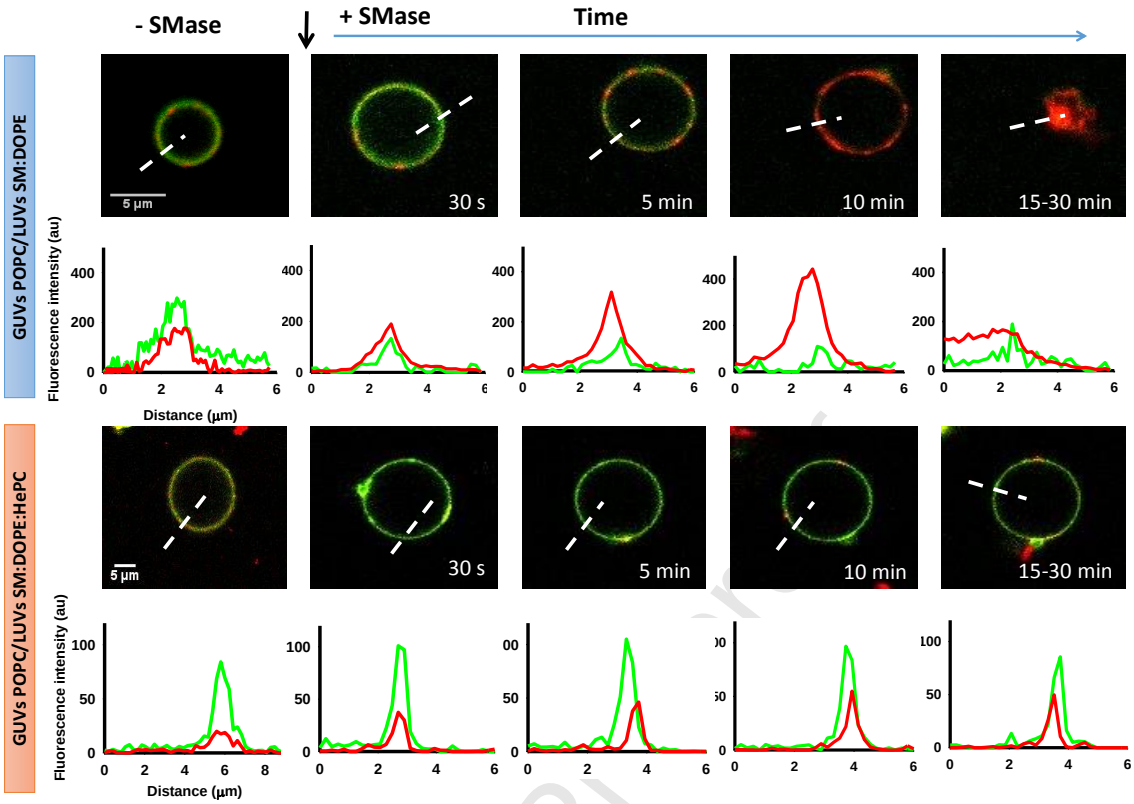

Figure 5: Confocal microscopy images of GUVs of POPC labeled with NBD-PE (green) and fusogenic Rho-PE-labeled LUVs (red) containing SM:DOPE (80:20) in the absence (upper panel) or presence (lower panel) of 20 mol% of HePC. The timestamps indicate the time after SMase addition. Fluorescence intensity profiles for the green and red channel in the GUV regions along the dashed lines are plotted under each image. Samples were excited at the NBD-PE excitation λ and images show the overlay of NBD-PE and Rho-PE emission channels.

After 10 min incubation time, the acceptor emission signal reached intensity values 25-30 higher than the donor emission (Figure 6B). At 30 min of enzyme treatment, microscopy images showed the presence of amorphous lipid clusters coming from collapsed GUVs, as well as an increase of GUVs aggregated in groups (see Figure S2). The LUV/GUV mixed solution in the absence of SMase, or in the presence of SMase + 100 mM EDTA, was stable over 30 min (Figure S2).

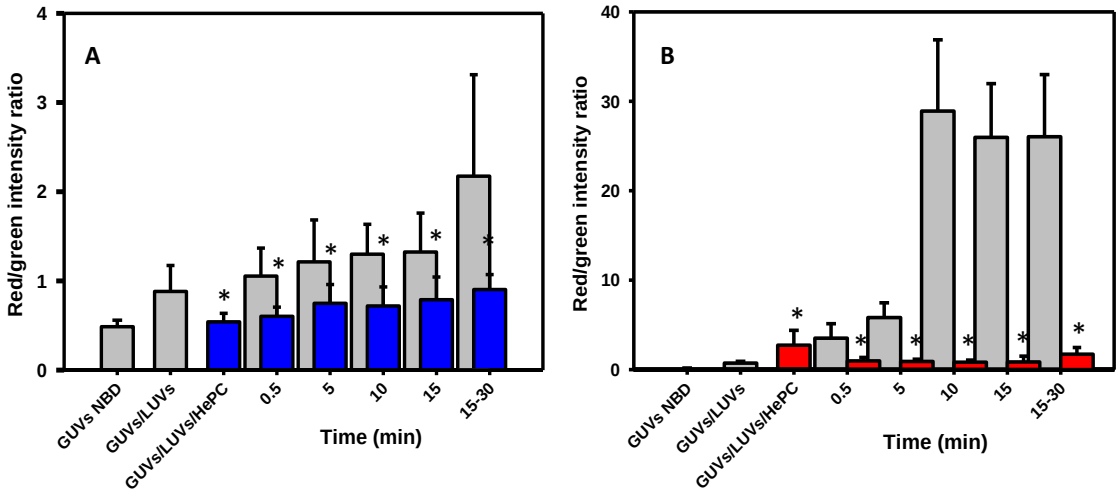

Figure 6: Semiquantitative analysis of fluorescence intensity of red/ green channels ratio for images of GUVs composed of POPC or SM/NBD-PE, and fusogenic LUVs labeled with Rho-PE over time. Vesicles composed of DOPC:DOPE (A) or SM:DOPE (B) in the absence (gray bars) or presence (blue or red bars) of 20 mol% of HePC were incubated with GUVs and PLC (A) or SMase (B) and analyzed over the reaction time. As a control, GUVs labeled with NBD-PE were included. n >30 GUVs were analyzed for each condition. Error bars correspond to SD. * indicates statistical differences of data obtained in similar conditions in the absence and presence of HePC with P <0.0001.

GUV collapse has been reported in vesicles subjected to the enzyme production of CER with very-long-chain polyunsaturated fatty acids [35]. Notably, in the present study, this membrane restructuring occurred in a trans-configuration, involving the production of CER in the LUVs, lipid transfer to GUV membranes and finally bilayer destabilization. The addition of 20 mol% of HePC reduced GUV destabilization after SMase treatment of the LUV/GUV mixed system (Figure 5 and vodeo_SMase_HePC), showing a slight increase in the red/green fluorescence ratio (Figure 6B), only isolated red dots on the GUV surface and a reduction of GUV aggregation in clusters (Figure S2).

4. Discussion

Our results indicate that HePC does not significantly influence the initial rate of reactions catalyzed by PLC or SMase. However, the extent of hydrolysis is inhibited by HePC over longer times. This effect was interpreted as a consequence of the inhibition of the membrane restructuring that allows full catalytic activity for PLC [53] and SMase [55,56]. In this work, we used SMase from a bacterial source, *Bacillus cereus*, and porcine pancreatic PLC because of its availability and extensive use in similar studies by other authors [46]. This might hamper the extrapolation of our results to a eukaryotic cellular environment due to differences in the catalytic mechanism and regulation properties of those enzymes with their intracellular counterparts. However, the effect of the accumulation of the DAG and CER products in biomembranes is expected to have similar consequences on the alteration of the physical properties of the membranes, regardless of their origin [33,37,57–59].

Phospholipases such as PLC and SMase act on the external hemilayer of vesicles, and access of the enzyme to the substrates located in the inner hemilayer is impaired. In this picture, membrane restructuring with the occurrence of nuclei of non-lamellar phases allows not only access to all the substrate population [56], but also permits the lipid product to dissipate into both hemilayers, reducing inhibition by product. The hindering of this membrane restructuring by HePC has in turn a dampening effect on enzyme hydrolysis over longer times.

This complex landscape is reflected in previous reports where HePC affects several phospholipases differently. HePC has been found to inhibit PLC [60,61] but not phospholipase D or SMase [62]. Furthermore, those authors reported differential regulation of phospholipase A_2 (PLA_2) by HePC, which cannot be explained by changes in membrane composition [63]. This suggests that phospholipase regulation should be understood in a non-classical way, taking into account not only the biochemical aspects but also the biophysical properties of the host membrane and its bi-directional regulation with enzyme activity [18,21,26,42,43].

As commented above, the phospholipase-driven catalytic process occurs asymmetrically, since these enzymes act only on the outer hemilayer of the membrane. DAG and CER are lipids with a small polar head compared to the two bulky hydrocarbon chains of its hydrophobic region, giving it a general inverted cone geometry. When the kinetics of the production of those lipids is faster than the flip-flop dynamics, the resultant membrane is highly stressed and in a state far from its compositional and curvature balance [52]. GUVs subjected to the asymmetric action of SMase relax this frustration into the formation of highly curved vesicles associated with the mother GUV [34].

This whole panorama favors the aggregation of vesicles with the formation of intermediate structures with highly negative curvature, which relaxes the geometric tension. Therefore, DAG and CER, as well as PE, are considered fusogenic molecules acting by stabilizing those highly curved membrane regions and promoting fusion events [33,35].

Whist HePC mechanism of action clearly involves cell membrane alteration [2], how this alteration propagates to the final target enzymes involved in lipid homeostasis and cell signaling is still under debate. Liquid-ordered (LO) nanodomains enriched in sterols and sphingolipids, named "lipid rafts" occur in living cell membranes and regulate important cell functions. Some authors have reported alkylphospholipids involvement in lipid raft stability, metabolism and apoptosis [2,9]. On the other hand, previous works from our laboratory evidenced that the presence of HePC destabilizes LO domains in cholesterol/phospholipid monolayers [12]. In agreement, Castro et al. concluded that the mechanism of action of alkylphospholipids is unlikely to be directly linked to alterations of lipid rafts biophysical properties caused by these drugs [31].

Taking into account the discrepancy on the effect of HePC on the lateral segregation of lipids, we explored a different aspect of membrane alteration, which involves membrane curvature stress modulation, following Dymond et al. predictions [28]. The results shown in this work robustly demonstrate that HePC inhibits membrane restructuring events, characteristic of the enzyme formation process of DAG and CER. HePC is a single-tailed alkylphospholipid analog that has an effective cone-shaped geometry (and a low critical parameter of Pc = 0.29) [12], which when

inserted into the bilayers can induce a positive curvature, counteracting the effect caused by DAG or CER. Therefore, HePC relaxes the curvature-tension of the enzymatically-treated membranes and restricts bilayer destabilization. It impedes those signaling messengers from diffusing laterally with continuity towards the membranes of other vesicles. It is worth noting that our results show that HePC inhibits the shape remodeling of lipid membranes which are not enzyme-substrate but interact with enzyme-treated vesicles. Thus, the effect of HePC influences cascades of events that overcome the local environment of enzyme activity.

This work focused on the action of HePC on two structurally unrelated enzymes, which degrade structurally different lipids (glycerol and sphingophospholipids), having in common that the products contain small polar groups and inverted cone structures. However, our results suggest that HePC may act in a non-classical way, and may influence not only those two enzymes but a greater variety of membrane-bound enzymes sensitive to curvature stress [16,18,19,21]. A recent report highlights the relationship between membrane curvature elastic stress and phospholipid homeostasis [18], the main target of HePC action in cells. Notably, HePC-resistant L*eishmania* promastigotes and HePC transiently treated parasites show a modification in their membrane lipid profile [6,10]. This lipid regulation may have the capacity to compensate for the non-specific alteration of the intrinsic curvature of the membrane caused by HePC.

In summary, the results reported in this work contribute to understanding the mechanism of action by which HePC regulates lipid metabolism and the transduction pathways of signals and offers evidence of a more holistic effect of HePC.

5. Acknowledgments

This work was supported by the Consejo Nacional de Investigaciones Científicas y Técnicas (CONICET), Agencia Nacional de Promoción Científica y Tecnológica (ANPCyT, FONCyT PICT 2017-0332 to MLF and PICT 2015-2575 to EEA), and the Secretary of Science and Technology of Universidad Nacional de Córdoba (SECyT-UNC), Argentina. Y.M.Z.D. is a CONICET fellow;

E.E.A. and M.L.F. are Career Investigators of CONICET-UNC. The microscopy experiments were performed at the "Centro de Micro y Nanoscopía de Córdoba" (CEMINCO-CIQUIBIC) working as part of the "Sistema Nacional de Microscopía (SNM)". The authors thank Dr. Carlos Mas and Dr. Cecilia Sampedro (CPA career-CONICET) for technical assistance in confocal microscopy image capture and analysis.

Author contributions: *Y.M. Zulueta Díaz*: Investigation, Validation, Formal Analysis, Visualization, Writing-review and editing. *E.E. Ambroggio*: Conceptualization, Supervision, Writing-review and editing. *M.L. Fanani*: Conceptualization, Supervision, Visualization, Writing – Original Draft, Project Administration, Resources, Funding Acquisition.

7. References

[1] S.L. Croft, J. Engel, Miltefosine — discovery of the antileishmanial activity of phospholipid derivatives, Trans. R. Soc. Trop. Med. Hyg. 100 (2006) S4–S8. https://doi.org/10.1016/j.trstmh.2006.03.009.

[2] W.J. Van Blitterswijk, M. Verheij, Anticancer Alkylphospholipids : Mechanisms of Action , Cellular Sensitivity and Resistance , and Clinical Prospects, Curr. Pharm. Des. 14 (2008) 2061–2074. https://doi.org/10.2174/138161208785294636.

[3] S.L. Croft, K. Seifert, V. Yardley, Current scenario of drug development for leishmaniasis, Indian J. Med. Res. 123 (2006) 399–410. https://doi.org/10.1016/j.trstmh.2006.03.009 Please.

[4] J. de Almeida Pachioni, J. Gallottini Magalhaes, E.J. Cardoso Lima, L. de Moura Bueno, J. Ferreira Barbosa, M. Malta de Sa, C. De Oliveira Rangel-Yagui, Alkylphospholipids - A promising class of chemotherapeutic agents with a broad pharmacological spectrum, J. Pharm. Pharm. Sci. 16 (2013) 742–759. https://doi.org/10.18433/J3CW23.

[5] T.P.C. Dorlo, M. Balasegaram, J.H. Beijnen, P.J. De Vries, Miltefosine: A review of its

pharmacology and therapeutic efficacy in the treatment of leishmaniasis, J. Antimicrob. Chemother. 67 (2012) 2576–2597. https://doi.org/10.1093/jac/dks275.

[6] M. Rakotomanga, S. Blanc, K. Gaudin, P. Chaminade, P.M. Loiseau, Miltefosine Affects Lipid Metabolism in Leishmania donovani Promastigotes, Antimicrob. Agents Chemother. 51 (2007) 1425–1430. https://doi.org/10.1128/AAC.01123-06.

[7] G. van Meer, D.R. Voelker, G.W. Feigenson, Membrane lipids : where they are and how they behave, Nat. Rev. 9 (2008) 112–124. https://doi.org/10.1038/nrm2330.

[8] P. Ríos-Marco, C. Marco, X. Gálvez, J.M. Jiménez-López, M.P. Carrasco, Alkylphospholipids: An update on molecular mechanisms and clinical relevance, Biochim. Biophys. Acta - Biomembr. 1859 (2017) 1657–1667. https://doi.org/10.1016/j.bbamem.2017.02.016.

[9] M. Saint-Pierre-Chazalet, B.M. Brahim, L. Le Moyec, C. Bories, M. Rakotomanga, P.M. Loiseau, Membrane sterol depletion impairs miltefosine action in wild-type and miltefosine-resistant Leishmania donovani promastigotes, J. Antimi. 65 (2009) 993–1001. https://doi.org/10.1093/jac/dkp321.

[10] M. Rakotomanga, M. Saint-Pierre-Chazalet, P.M. Loiseau, Alteration of fatty acid and sterol metabolism in miltefosine-resistant Leishmania donovani promastigotes and consequences for drug-membrane interactions, Antimicrob. Agents Chemother. 49 (2005) 2677–2686. https://doi.org/10.1128/AAC.49.7.2677-2686.2005.

[11] D.H. Beach, G.G. Holz, G.E. Anekwe, Lipids of Leishmania Promastigotes, J. Parasitol. 65 (1979) 203–216.

[12] Y.D.L.M. Zulueta Díaz, M.L. Fanani, Crossregulation between the insertion of Hexadecylphosphocholine (miltefosine) into lipid membranes and their rheology and lateral structure, Biochim. Biophys. Acta - Biomembr. 1859 (2017) 1891–1899. https://doi.org/10.1016/j.bbamem.2017.06.008.

[13] I.R. Gómez-Serranillos, J.J. Miñones, P. Dynarowicz-Łątka, J. Miñones, E. Iribarnegaray,

Miltefosine - Cholesterol Interactions : A Monolayer Study, Langmuir. 20 (2004) 928–933.

[14] J.M. Seddon, R.H. Templer, Polymorphism of Lipid-Water Systems, in: R.L. and E. Sackmann (Ed.), Handb. Biol. Phys., Elsevier Science B.V, London SW7, 1995: pp. 97–160.

[15] P. V. Escribá, Membrane-lipid therapy: A new approach in molecular medicine, Trends Mol. Med. 12 (2006) 34–43. https://doi.org/10.1016/j.molmed.2005.11.004.

[16] S.M. a Davies, R.M. Epand, R. Kraayenhof, R.B. Cornell, Regulation of CTP: Phosphocholine cytidylyltransferase activity by the physical properties of lipid membranes: An important role for stored curvature strain energy, Biochemistry. 40 (2001) 10522–10531. https://doi.org/10.1021/bi010904c.

[17] R.M. Epand, Lipid polymorphism and protein-lipid interactions, Biochim. Biophys. Acta - Rev. Biomembr. 1376 (1998) 353–368. https://doi.org/10.1016/S0304-4157(98)00015-X.

[18] M.K. Dymond, Mammalian phospholipid homeostasis: Evidence that membrane curvature elastic stress drives homeoviscous adaptation in vivo, J. R. Soc. Interface. 13 (2016). https://doi.org/10.1098/rsif.2016.0228.

[19] R.B. Cornell, R.S. Arnold, Modulation of the activities of enzymes of membrane lipid metabolism by non-bilayer-forming lipids, Chem. Phys. Lipids. 81 (1996) 215–227. https://doi.org/10.1016/0009-3084(96)02584-4.

[20] J.C. Bozelli, W. Jennings, S. Black, Y.H. Hou, D. Lameire, P. Chatha, T. Kimura, B. Berno, A. Khondker, M. Rheinstädter, R.M. Epand, Membrane curvature allosterically regulates the phosphatidylinositol cycle, controlling its rate and acyl chain composition of its lipid intermediates, J. Biol. Chem. 293 (2018) 17780–17791. https://doi.org/10.1074/jbc.RA118.005293.

[21] A.E. Drobnies, S.M. a Davies, R. Kraayenhof, R.F. Epand, R.M. Epand, R.B. Cornell, CTP:phosphocholine cytidylyltransferase and protein kinase C recognize different physical features of membranes: Differential responses to an oxidized phosphatidylcholine, Biochim. Biophys. Acta - Biomembr. 1564 (2002) 82–90. https://doi.org/10.1016/S0005-

2736(02)00404-2.

[22] P. V. Escribá, A. Ozaita, C. Ribas, A. Miralles, E. Fodor, T. Farkas, J.A. García-Sevilla, Role of lipid polymorphism in G protein-membrane interactions : Nonlamellar-prone phospholipids and peripheral protein binding, PNAS. 94 (1997) 11375–11380. https://doi.org/10.1073/pnas.94.21.11375.

[23] O. Vögler, J. Casas, D. Capó, T. Nagy, G. Borchert, G. Martorell, P. V Escribá, The G□□ Dimer Drives the Interaction of Heterotrimeric Gi Proteins with Nonlamellar Membrane Structures, J. Biol. Chem. 279 (2004) 36540–36545. https://doi.org/10.1074/jbc.M402061200.

[24] O. Vögler, J.M. Barceló, C. Ribas, P. V Escribá, Membrane interactions of G proteins and other related proteins, Biochim. Biophys. Acta - Biomembr. 1778 (2008) 1640–1652. https://doi.org/10.1016/j.bbamem.2008.03.008.

[25] M. Ibarguren, P.H.H. Bomans, P.M. Frederik, M. Stonehouse, A.I. Vasil, M.L. Vasil, A. Alonso, F.M. Goñi, End-products diacylglycerol and ceramide modulate membrane fusion induced by a phospholipase C/sphingomyelinase from Pseudomonas aeruginosa, Biochim. Biophys. Acta - Biomembr. 1798 (2010) 59–64. https://doi.org/10.1016/j.bbamem.2009.10.017.

[26] H. Ahyayauch, A. V Villar, A. Alonso, F.M. Goñi, Modulation of PI-Specific Phospholipase C by Membrane Curvature and Molecular Order, Biochemistry. 44 (2005) 11592–11600. https://doi.org/10.1021/bi050715k.

[27] P. V Escriba, M. Sastre, J.A. Garcia-sevilla, Disruption of cellular signaling pathways by daunomycin through destabilization of nonlamellar membrane structures, PNAS. 92 (1995) 7595–7599. https://doi.org/10.1073/pnas.92.16.7595.

[28] M. Dymond, G. Attard, A.D. Postle, Testing the hypothesis that amphiphilic antineoplastic lipid analogues act through reduction of membrane curvature elastic stress., J. R. Soc. Interface. 5 (2008) 1371–1386. https://doi.org/10.1098/rsif.2008.0041.

[29] B. Malheiros, Biophysical Characterization of cubosomal nanoparticles intended for drug delivery applications and its interaction with a model drug: the miltefosine case, UNIVERSIDADE DE SÃO PAULO – USP, 2018. https://doi.org/10.11606/D.9.2018.tde-18122018-172044.

[30] B. Heczková, J.P. Slotte, Effect of anti-tumor ether lipids on ordered domains in model membranes, FEBS Lett. 580 (2006) 2471–2476. https://doi.org/10.1016/j.febslet.2006.03.079.

[31] B.M. Castro, A. Fedorov, V. Hornillos, J. Delgado, A.U. Acuña, F. Mollinedo, M. Prieto, Edelfosine and Miltefosine Effects on Lipid Raft Properties: Membrane Biophysics in Cell Death by Antitumor Lipids, J. Phys. Chem. B. 117 (2013) 7929–7940. https://doi.org/10.1021/jp401407d.

[32] J. Miñones, S. Pais, J. Miñones, O. Conde, P. Dynarowicz-Łatka, Interactions between membrane sterols and phospholipids in model mammalian and fungi cellular membranes - A Langmuir monolayer study, Biophys. Chem. 140 (2009) 69–77. https://doi.org/10.1016/j.bpc.2008.11.011.

[33] F.M. Goñi, L.R. Montes, A. Alonso, Phospholipases C and sphingomyelinases: Lipids as substrates and modulators of enzyme activity, Prog. Lipid Res. 51 (2012) 238–266. https://doi.org/10.1016/j.plipres.2012.03.002.

[34] J.M. Holopainen, M.I. Angelova, P.K. Kinnunen, Vectorial budding of vesicles by asymmetrical enzymatic formation of ceramide in giant liposomes., Biophys. J. 78 (2000) 830–838. https://doi.org/10.1016/S0006-3495(00)76640-9.

[35] D.A. Peñalva, S.S. Antollini, E.E. Ambroggio, M.I. AveldanÌo, M.L. Fanani, Membrane Restructuring Events during the Enzymatic Generation of Ceramides with Very Long-Chain Polyunsaturated Fatty Acids, Langmuir. 34 (2018) 4398–4407. https://doi.org/10.1021/acs.langmuir.7b04374.

[36] F.M. Goñi, A. Alonso, Membrane fusion induced by phospholipase C and

sphingomyelinases, Biosci. Rep. 20 (2000) 443–463. https://doi.org/10.1023/A:1010450702670.

[37] W.J. van Blitterswijk, A.H. van der Luit, R.J. Veldman, M. Verheij, J. Borst, Ceramide: second messenger or modulator of membrane structure and dynamics?, Biochem. J. 369 (2003) 199–211. https://doi.org/10.1042/BJ20021528.

[38] R. Pankov, T. Markovska, P. Antonov, L. Ivanova, A. Momchilova, The plasma membrane lipid composition affects fusion between cells and model membranes, Chem. Biol. Interact. 164 (2006) 167–173. https://doi.org/10.1016/j.cbi.2006.09.010.

[39] Y. Zhang, X. Li, K.A. Becker, E. Gulbins, Ceramide-enriched membrane domains-Structure and function, Biochim. Biophys. Acta - Biomembr. 1788 (2009) 178–183. https://doi.org/10.1016/j.bbamem.2008.07.030.

[40] F.M. Goñi, A. Alonso, Sphingomyelinases: Enzymology and membrane activity, FEBS Lett. 531 (2002) 38–46. https://doi.org/10.1016/S0014-5793(02)03482-8.

[41] P.Y. Quartino, G.D. Fidelio, J.B. Manneville, B. Goud, E.E. Ambroggio, Detecting phospholipase activity with the amphipathic lipid packing sensor motif of ArfGAP1, Biochem. Biophys. Res. Commun. 505 (2018) 290–294. https://doi.org/10.1016/j.bbrc.2018.09.116.

[42] B. Maggio, G. a. Borioli, M. Boca, L. Tullio, M.L. Fanani, R.G. Oliveira, C.M. Rosetti, N. Wilke, Composition-driven Surface Domain Structuring Mediated by Sphingolipids and Membrane-active Proteins, Cell Biochem. Biophys. 50 (2008) 79–109. https://doi.org/10.1007/s12013-007-9004-1.

[43] M.L. Fanani, S. Hartel, B. Maggio, L. De Tullio, J. Jara, F. Olmos, R.G. Oliveira, The action of sphingomyelinase in lipid monolayers as revealed by microscopic image analysis, Biochim. Biophys. Acta - Biomembr. 1798 (2010). https://doi.org/10.1016/j.bbamem.2010.01.001.

[44] M.B. Ruiz-Argüello, M.P. Veiga, J.L.R. Arrondo, F.M. Goñi, A. Alonso, Sphingomyelinase

cleavage of sphingomyelin in pure and mixed lipid membranes. Influence of the physical state of the sphingolipid, Chem. Phys. Lipids. 114 (2002) 11–20. https://doi.org/10.1016/S0009-3084(01)00195-5.

[45] J.A. Bellon, M.J. Pino, N. Wilke, Low-cost equipment for electroformation of Giant Unilamellar Vesicles, HardwareX. 4 (2018) e00037. https://doi.org/10.1016/j.ohx.2018.e00037.

[46] M.B. Ruiz-Alguello, G. Basañez, M.F. Goñi, A. Alonso, Different effects of enzyme-generated ceramides and diacylglycerols in phospholipid membrane fusion and leakage, J. Biol. Chem. 271 (1996) 926616–26621. https://doi.org/10.1016/S0079-6107(97)80314-8.

[47] J.L. Nieva, F.M. Goñi, A. Alonso, Liposome Fusion Catalytically Induced by Phospholipase C, Biochemistry. 28 (1989) 7364–7367. https://doi.org/10.1021/bi00444a032.

[48] F. Ogushi, R. Ishitsuka, T. Kobayashi, Y. Sugita, Rapid flip-flop motions of diacylglycerol and ceramide in phospholipid bilayers, Chem. Phys. Lett. 522 (2012) 96–102. https://doi.org/10.1016/j.cplett.2011.11.057.

[49] M.L. Fanani, B. Maggio, Kinetic steps for the hydrolysis of sphingomyelin by Bacillus cereus sphingomyelinase in lipid monolayers, J. Lipid Res. 41 (2000).

[50] I.R. Miller, J.M. Ruysschaert, Enzymic activity and surface inactivation of phospholipase C at the water/air interface, J. Colloid Interface Sci. 35 (1971) 340–345. https://doi.org/10.1016/0021-9797(71)90128-7.

[51] R.B. Lira, R. Dimova, Fusion assays for model membranes: a critical review, in: Adv. Biomembr. Lipid Self-Assembly, Elsevier, 2019: pp. 229–270. https://doi.org/10.1016/bs.abl.2019.09.003.

[52] I. López-Montero, M. Vélez, P.F. Devaux, Surface tension induced by sphingomyelin to ceramide conversion in lipid membranes, Biochim. Biophys. Acta - Biomembr. 1768 (2007) 553–561. https://doi.org/10.1016/j.bbamem.2007.01.001.

[53] G. Basáñez, J.L. Nieva, F.M. Goñi, A. Alonso, Origin of the lag period in the phospholipase

C cleavage of phospholipids in membranes. Concomitant vesicle aggregation and enzyme activation, Biochemistry. 35 (1996) 15183–15187. https://doi.org/10.1021/bi9616561.

[54] R.B. Lira, T. Robinson, R. Dimova, K.A. Riske, Highly Efficient Protein-free Membrane Fusion: A Giant Vesicle Study, Biophys. J. 116 (2019) 79–91. https://doi.org/10.1016/j.bpj.2018.11.3128.

[55] S.N. Pinto, E.L. Laviad, J. Stiban, S.L. Kelly, A.H. Merrill, M. Prieto, A.H. Futerman, L.C. Silva, Changes in membrane biophysical properties induced by sphingomyelinase depend on the sphingolipid N-acyl chain., J. Lipid Res. 55 (2014) 53–61. https://doi.org/10.1194/jlr.M042002.

[56] L.C. Silva, A.H. Futerman, M. Prieto, Lipid raft composition modulates sphingomyelinase activity and ceramide-induced membrane physical alterations, Biophys. J. 96 (2009) 3210–3222. https://doi.org/10.1016/j.bpj.2008.12.3923.

[57] I. López-Montero, F. Monroy, M. Vélez, P.F. Devaux, Ceramide: From lateral segregation to mechanical stress, Biochim. Biophys. Acta - Biomembr. 1798 (2010) 1348–1356. https://doi.org/10.1016/j.bbamem.2009.12.007.

[58] J.C. Gómez-Fernández, S. Corbalán-García, Diacylglycerols, multivalent membrane modulators, Chem. Phys. Lipids. 148 (2007) 1–25. https://doi.org/10.1016/j.chemphyslip.2007.04.003.

[59] A. Alonso, F.M. Goñi, The Physical Properties of Ceramides in Membranes, Annu. Rev. Biophys. 47 (2018) Epub ahead of print. https://doi.org/10.1146/annurev-biophys-070317-033309.

[60] D. Berkovic, M. Goeckenjan, S. Lüders, W. Hiddemann, E.A. Fleer, Hexadecylphosphocholine inhibits phosphatidylinositol and phosphatidylcholine phospholipase C in human leukemia cells, J. Exp. Ther. Oncol. 1 (1996) 302—311.

[61] M.J. Wargo, M.J. Gross, S. Rajamani, J.L. Allard, L.K.A. Lundblad, G.B. Allen, M.L. Vasil, L.W. Leclair, D.A. Hogan, Hemolytic phospholipase C inhibition protects lung function

during Pseudomonas aeruginosa infection, Am. J. Respir. Crit. Care Med. 184 (2011) 345–354. https://doi.org/10.1164/rccm.201103-0374OC.

[62] D. Berkovic, K. Berkovic, C. Binder, D. Haase, E.A.M. Fleer, Hexadecylphosphocholine does not influence phospholipase D and sphingomyelinase activity in human leukemia cells, J. Exp. Ther. Oncol. 2 (2002) 213–218. https://doi.org/10.1046/j.1359-4117.2002.01036.x.

[63] D. Berkovic, S. Lüders, M. Goeckenjan, W. Hiddemann, E.A.M. Fleer, Differential regulation of phospholipase A2 in human leukemia cells by the etherphospholipid analogue hexadecylphosphocholine, Biochem. Pharmacol. 53 (1997) 1725–1733. https://doi.org/10.1016/S0006-2952(97)00095-6.

Declaration of interests

☒ The authors declare that they have no known competing financial interests or personal relationships that could have appeared to influence the work reported in this paper.

☐The authors declare the following financial interests/personal relationships which may be considered as potential competing interests:

Graphical abstract

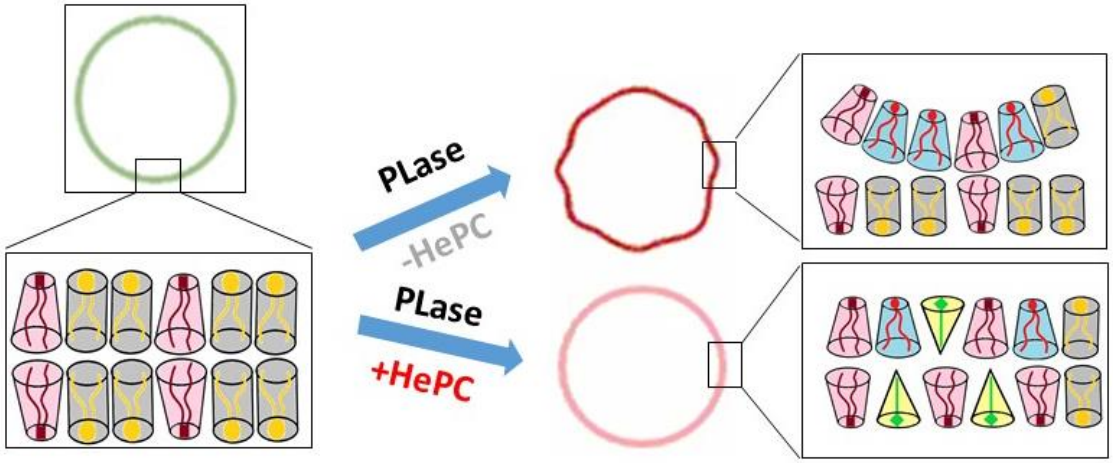

Highlights

- Miltefosine (hexadecylphosphocholine or HePC) alters phospholipases action.
- HePC inhibits diacylglycerol and ceramide-induced liposome aggregation.
- HePC inhibit membrane fusion induced by phospholipase C and sphingomyelinase action
- HePC would act through relaxation of membrane curvature stress